공학석사학위논문

Effect of poly(methyl methacrylate) particles on the initiation of instability in the capillary thinning of poly(ethylene oxide) solution

PEO 용액 신장 시 발생하는 불안정 거동에 PMMA 입자가 미치는 영향에 관한 연구

2018년 2월

서울대학교 대학원
화학생물공학부
옥 장 훈

Effect of poly(methyl methacrylate) particles on the initiation of instability in the capillary thinning of poly(ethylene oxide) solution

PEO용액 신장 시 발생하는 불안정 거동에 PMMA 입자가 미치는 영향에 관한 연구

지도교수 **안 경 현**

이 논문을 공학석사학위논문으로 제출함
2018년 2월

서울대학교 대학원
화학생물공학부
옥 장 훈

옥장훈의 석사학위논문을 인준함
2017년 12월

위 원 장 _____(인)

부위원장 _____(인)

위 원 _____(인)

Abstract

Effect of poly(methyl methacrylate) particles on the initiation of instability in the capillary thinning of poly(ethylene oxide) solution

Ock, Janghoon

School of Chemical and Biological Engineering

The Graduate School

Seoul National University

The effect of particles on the instability in the capillary thinning process of poly(ethylene oxide) solution has been experimentally studied to further understand the filament breakup behavior of the particulate systems. We focus on breathing and the formation of the 1st bead, in particular, which initiates blistering. The change in instability pattern by the added PMMA particles is investigated by observing the evolution of the filament undergoing capillary thinning. Addition of particles accelerates breathing and the formation of the 1st bead. By comparing the extensional properties of PMMA/PEO suspension with that of Glycerin/PEO solutions which has the same viscosity, surface tension and polymer concentration, we confirm that the early occurrence of the instability is ascribed to the inhibition on chain

extension due to the presence of particles. The addition of particles has an influence on the position of the 1st bead. For a pure polymer solution and polymer solution with a small amount of particles (~2 wt%), the 1st bead mostly appears near the upper neck. However, as the particle concentration increases up to 10 wt%, the 1st bead is formed anywhere along the filament with similar probability. The randomization of the position of the 1st bead is attributed to the non-uniform distribution of particles inside a filament by the fluctuation of the local particle concentration.

Keywords: Instability, Capillary thinning, Filament breakup, Extensional flow, PMMA/PEO suspension

Student Number: 2016 - 21038

Contents

List of Figures

List of Tables

1. Introduction

Material processing can be understood based on a single platform which is called ‘transport phenomena of complex fluids’ [1]. During processing, fluids experience complex flow fields combining shear and extensional flow. In several processes such as coating [2, 3], printing [4], mixing [5], spraying [3], and spinning [6], extensional flow is a dominant flow type against shear. In order to precisely understand such processes, it is essential to apprehend the behavior of materials under extensional flow. Polymeric liquids present complex instability patterns under extensional flow, such as beads-on-a-string (BOAS) structure, formation of satellites and nano-fibers, right before the final break-up [7-9]. For particulate suspensions, the added particles induce acceleration of final break-up velocity, rough free surface, and random pinch-off behavior [10-13].

The extensional behavior of fluids can be examined by using the capillary thinning rheometry, in which the extensional deformation is applied on a small amount of fluid loaded between two plates by lifting the upper plate [14]. During the elongating process, inertia, viscous and elastic stress resist against capillary pressure which tends to break the liquid bridge between the two plates. The dynamics of thinning liquid bridge is determined by the balance among these forces. The thinning process is called capillary thinning or capillarity-induced thinning, which is a self-thinning process that depends only on the properties of the fluid without any involvement of external forces. The capillary thinning process of polymer solution is divided into three stages before the final break-up [15-17]. Firstly, in Newtonian stage, the thinning

dynamics is determined by the balance between capillary pressure and a combination of inertia and viscous stress because the elastic stress is not actively involved in the thinning process due to small deformation. In other words, the thinning dynamics in this stage follows that of a Newtonian fluid. Next, in elasto-capillary stage, the elastic stress which originates from the extension of polymer chain under extensional flow resists against the capillary pressure. At the moment the second stage begins, a cylindrical filament where uniaxial extensional flow is predominant is formed between upper and lower drops, and its diameter decreases exponentially with time. Lastly, in instability stage, the filament stops decaying exponentially and the iterated beads appear, inducing perturbation of the free surface. The successive outbreak of iterated beads is called “blistering,” and the beads-on-a-string (BOAS) is a representative structure.

As the instability on the surface is directly involved in the final break-up of the fluid, it has been intensively studied. Oliveira and McKinley [18] experimentally demonstrated the dynamics of blistering of viscoelastic fluids. By visualizing the capillary thinning process of polymer solutions, they elaborated the correlation of the exponential decay of the thinning filament, the occurrence of iterated beads, and their coalescence. There was a simulation which predicts the formation of BOAS structure and the exponential decay of the filament [19]. By using Oldroyd-B and FENE model, it was demonstrated that polymer chain recoils inside the satellite beads of BOAS structure and the filament finally ruptures when the polymer chain reaches its finite extensibility. Sattler et al. [20] detailed types of instability, reporting “breathing” - the constriction at the neck connecting the filament and

liquid drop - by observing the evolution of free surface of the filament. The polymer chains, highly stretched by strong extensional flow inside the filament, shrink to the relaxed state in the drop where the flow disappears. A slight constriction takes place at the neck where the elastic stress cannot sufficiently resist against the capillary pressure with the transition of the polymer chain conformation. It also arouses the difference in capillary pressure between the neck and the filament, which induces the formation of beads. Thus, breathing which becomes evident almost at the end of the elasto-capillary stage triggers the blistering of which initiation can be noticed by the formation of the 1st bead. Previous studies mostly focused on the blistering pattern at the capillary thinning of pure polymer solutions which do not include particles. Meanwhile, although particulate systems such as battery slurry, printed electronics and paint, are more valuable industrial materials for the extension-dominant processes [2-6, 21, 22], few studies have carried out with the particulate polymer solutions because of the complexity. The heterogeneity of the system expected to induce complex behavior different from pure polymer solutions [23, 24]. Han and Kim [25] demonstrated that for the particulate system the extension of polymer chain under extensional flow was suppressed by the shear flow component at the particle surface due to no slip boundary condition. The non-uniformity in the flow due to the presence of particles can affect the chain conformation of polymers, suggesting that it might alter the instability pattern.

To thoroughly understand the extensional behavior of complex fluids consisting of particles and polymers, it is important to consider the effect of particles on the fluid properties and how the fluid

properties change the instability. Studies on the extensional behavior of particulate polymer solutions have been mainly performed on the thinning dynamics and behavior of polymer and particles under flow, not on the instability pattern. In this study, the effect of particles on the initiation of the instability, which leads to the final break-up, was investigated. For this purpose, the filament undergoing capillary thinning process was focused so as to investigate the change in the breathing and the 1^{st} bead formation which initiate blistering. By analyzing images of capillary thinning process of which the time spacing is 0.25 ms, the effect of particles on the outbreak of the instability was scrutinized.

2. Experiments

2.1. Material

Poly(methyl methacrylate) (PMMA) particles were dispersed in poly(ethylene oxide) (PEO, Sigma-Aldrich, Mw = 2,000,000 g/mol) solution to make a model system of PMMA/PEO suspension. The PMMA particles (Sekisui Plastics, Japan) were monodisperse and spherical, and the diameter was 1 μm. The density of the particles is 1.18 g/cm^3. PMMA particles were dispersed in distilled water by sonication for 30 min, and then 1 wt% master PEO solution was added to the suspension with pre-calculated amount while stirred gently with magnetic stirrer so as to make well-dispersed PMMA/PEO suspensions. PEO concentration was 0.5 wt% for all samples and PMMA particle concentration was varied with 2, 5, 8, 10 wt%, with labels of PEO0.5_PM2, PEO0.5_PM5, PEO0.5_PM8 and PEO0.5_PM10, respectively. In order to prevent sedimentation and maintain the well-dispersed state, the samples were continuously stirred with magnetic stirrer and only a small amount of sample was taken by a pipette to conduct the extension test.

The viscosity was measured by AR-G2 (TA instruments, USA) with a 60 mm parallel plate at 25℃. The extensional relaxation time was extracted from the time evolution of filament diameter, which was obtained from the shadowgraph images of capillary thinning process. A tensiometer DCAT-21 (Data Physics Instruments, Germany) was employed to measure the surface tension using the plate method. All properties of sample fluid are shown in Table 1.

Table 1. Properties of PMMA/PEO suspensions; $\boldsymbol{\phi_p}$ is the particle weight fraction, $\boldsymbol{\eta_0}$ is the zero-shear viscosity, $\boldsymbol{\lambda_e}$ is the extensional relaxation time, and $\boldsymbol{\sigma}$ is the surface tension

Name	**PEO conc. [wt%]**	$\boldsymbol{\phi_p}$ $[wt\%]$	$\boldsymbol{\eta_0}$ $[cP]$	$\boldsymbol{\lambda_e}$ $[ms]$	$\boldsymbol{\sigma}$ $[mN/m]$
PEO0.5	0.5	0	19.9	11.02	59.55
PEO0.5_PM2		2	20.7	12.34	58.95
PEO0.5_PM5		5	23.2	12.97	57.99
PEO0.5_PM8		8	27.4	13.41	57.37
PEO0.5_PM10		10	31.6	14.07	57.31

2.2. Experimental setup

Extensional deformation was applied on the loaded fluid by a modified universal testing machine (UTM; LF plus, Lloyd Instruments, UK) setup to induce capillary thinning. Details of this setup with a high-speed camera and halogen lamp were described in Fig.1. A small amount of sample was loaded between the two plates with a diameter of 3 mm and the upper plate was lifted with a rate of 0.5 mm/s. An initial gap between the two plates was set as 1.5 mm which is smaller than the capillary length ($l_{cap} = \sqrt{\sigma/\rho g} \approx 2.47\,mm$, σ : surface tension of the fluid ρ : density of the fluid) to prevent gravitational sagging [26].

In the elasto-capillary stage of capillary thinning, a polymeric filament is formed between upper and lower drops, and its diameter decreases exponentially over time following Eq (1) [14].

$$\frac{D(t)}{D_0} = \left(\frac{G}{4\sigma/D_0}\right)^{1/3} \exp(-t/3\lambda_e) \quad (1)$$

where G is the elastic modulus, σ is the surface tension of the fluid, λ_e is the extensional relaxation time, and D_0 is the initial diameter of exponentially decaying filament.

The flow inside the filament is uniaxial extensional flow and its extension rate ($\dot{\varepsilon}$) can be derived from the time evolution of diameter according to Eq (2). As the diameter of the filament decays exponentially in the elasto-capillary stage, the extension rate remains constant.

$$\dot{\varepsilon} = -\frac{2}{D(t)} \frac{dD(t)}{dt} \tag{2}$$

The apparent extensional viscosity (η_E) is defined as;

$$\eta_E = -\frac{\sigma}{dD(t)/dt} = \frac{2\sigma}{D(t) \cdot \dot{\varepsilon}(t)} \tag{3}$$

The extensional properties were calculated from the time evolution of filament diameter, which was extracted by visualizing the capillary thinning process. Extensional flow with $\dot{\varepsilon} = 30{\sim}60\ s^{-1}$ was generated inside the filament. The diameter of the filament was several tens of micrometers, and it took only decades of milliseconds to reach the final break-up. A high-speed camera (Photron Fastcam Ultima 512, Photron, USA) was used to visualize such a rapid process. The whole process was recorded to obtain shadowgraph image sequences of thinning filament by using a high-speed camera equipped with a high magnification lens (X5,10,20 objective lens, X12 adaptor). During the process, the backlight illumination was provided by a 250W halogen lamp (BMH-250, Mejiro precision, Japan) as in Fig.1. Three types of objective lenses with different magnification (X5, 10, and 20) were used for different target observing area. One pixel of the image covers 2.88, 1.97, 0.97 μm, respectively. The high-speed camera took 2000 and 4000 frames per second at a resolution of 512 × 512, 256 × 512 pixels, respectively. We obtained the time evolution of the filament by detecting the edge of free surface of the filament, from which the extensional properties were extracted.

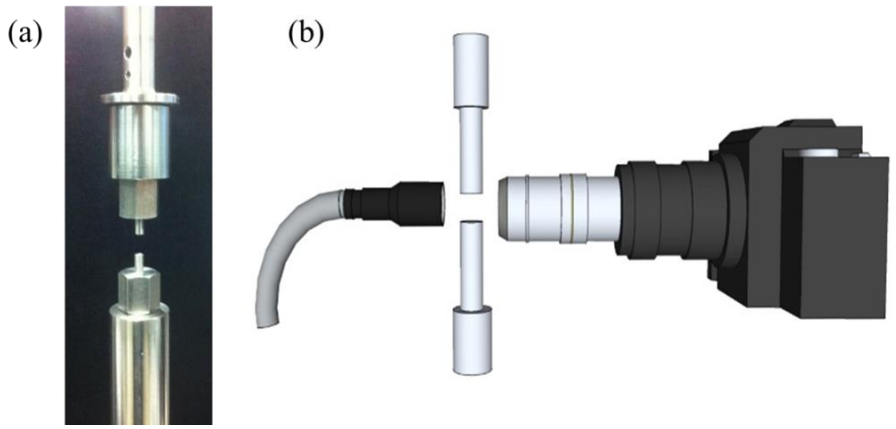

Figure 1. Experimental setup: (a) modified section of UTM; (b) a schematic of the modified UTM and visualization setup

2.3. Dimensionless numbers

2.3.1. Elasto-capillary number

The elasto-capillary number (Ec), a ratio of the Weissenberg number (Wi) and the capillary number (Ca), can characterize the free surface flow of an elastic fluid [27, 28].

$$\mathrm{Ec} \equiv \frac{Wi}{Ca} = \frac{\lambda\sigma}{\eta_0 R} \tag{4}$$

where λ is the relaxation time, σ is the surface tension, η_0 is the zero shear viscosity, R is the radius of the filament.

In the elasto-capillary stage where a polymeric filament is formed, the Elasto-capillary number was calculated as 470~560. Non-Newtonian effect which results from the elastic stress generated by stretching polymer chains dominates the thinning dynamics in the elasto-capillary stage.

2.3.2. Progression of capillary thinning

In general, the capillary thinning process is presented with diameter change over time in logarithmic scale so as to highlight the exponential decay of the filament in the elasto-capillary stage which lasts the longest among the three stages. The constant extension rate in the elasto-capillary stage, which determines the characteristic process time, is extracted from the diameter change over time. Once the blistering takes place in the instability stage, however, it is not able to observe the capillary thinning process simply from the relationship between time and diameter because of the perturbation of the free surface. Thus, a dimensionless parameter, t^*, which refers to the progression of capillary thinning, was introduced to compare the instability stage of different capillary thinning processes with considering the characteristic process time of each process [29].

$$t^* = \frac{t}{3\lambda_e} \tag{5}$$

Fig.2 shows the capillary thinning process of 0.50 and 0.75 wt% PEO solutions. Newtonian stage was significantly short due to the low extensional viscosity of samples. In the elasto-capillary stage of which the initiation was denoted as $t = 0$, the exponential decay of the filament is plotted in the form of $\log D(t) = a - bt$ (Fig.2 (a)). Extensional relaxation time (λ_e) was derived from the slope (b) of the plot with $\lambda_e = 1/3b$. The slopes for PEO 0.5 and 0.75 wt% are 30.4 and 18.2 s^{-1}, respectively, and the extensional relaxation time calculated from the slope are 10.96 and 17.31 ms, respectively. Three times the extensional relaxation time, $3\lambda_e = \Delta t/\Delta \log D$, can be calculated from the combination of $b = \Delta \log D/\Delta t$ and $\lambda_e = 1/3b$.

As Δt is proportional to duration of the elasto-capillary stage, $3\lambda_e$ was defined as a characteristic process time of the capillary thinning process [17, 26]. Thus, by normalizing the real time (t) with $3\lambda_e$, we can see the elapse of time relative to the characteristic process time, i.e. the progression of capillary thinning (Fig.2 (b)). As shown in Fig.2 (a), extension rate was varied with polymer concentration and the thinning process proceeded with different rate for each sample. On the other hand, by normalizing time with $3\lambda_e$, two different capillary thinning process plots overlapped into a single plot, allowing a comparison with a single standard. The instability took place approximately 80 and 125 ms after the elasto-capillary stage had begun at $t = 0$, respectively, for PEO 0.50 and 0.75 wt% solution. Though the instability stage begins at different points on the real time basis (Fig.2 (a)), they start off almost at the same point ($t^* = 2.40$) on the basis of t^*, which represents the progression of capillary thinning process (Fig.2 (b)). Likewise, introduction of t^* allows the comparison of the stage transition in different capillary thinning processes with a single parameter.

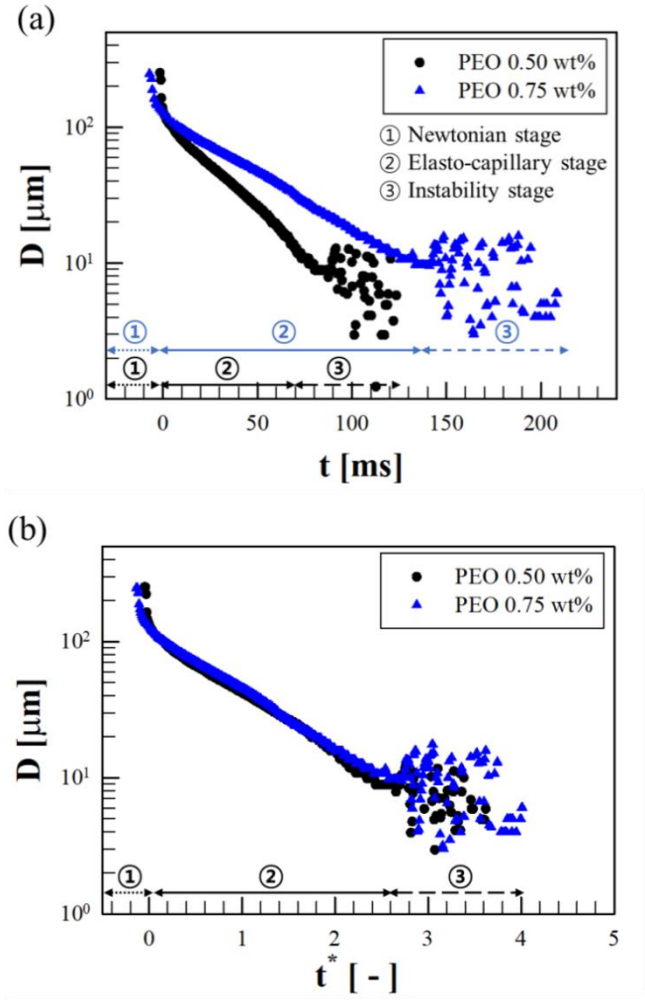

Figure 2. Evolution of filament diameter (***D***) at different PEO (Mw = 2,000,000) concentration; 0.50, 0.75 wt%: (a) as a function of real time (***t***); (b) as a function of the progression of capillary thinning (t^*). The point at which the elasto-capillary stage begins is set as $t = 0$. Each stage is denoted with number in numerical order.

3. Results and discussion

3.1. PMMA/PEO suspensions

3.1.1. The property of the bulk fluid

We investigated the effect of particles on the instability which appeared under extensional flow by observing the capillary thinning process of PEO solutions with well-dispersed PMMA particles. First of all, the properties of the suspensions were characterized by measuring shear viscosity and extensional relaxation time. In order to solely investigate the effect of particles, the concentration of polymer was kept constant. Addition of particles incurs the change in properties of the bulk fluid. The viscosity (Fig.3 (a)) and the extensional relaxation time (Fig.3 (b)) of the suspensions increased with particle concentration. Although the surface tension dropped slightly by 1 ~ 3%, it was not a significant change (Table 1). In order to confirm that polymer concentration was kept constant during the test, the amount of free polymer in the medium was determined after the extension test by measuring the mass of the remnants after removing the fluid by centrifuge. It turned out that there was little change in the amount of free polymer in the medium. PEO did not adsorb on PMMA particles and there was no polymer degradation during the experiment.

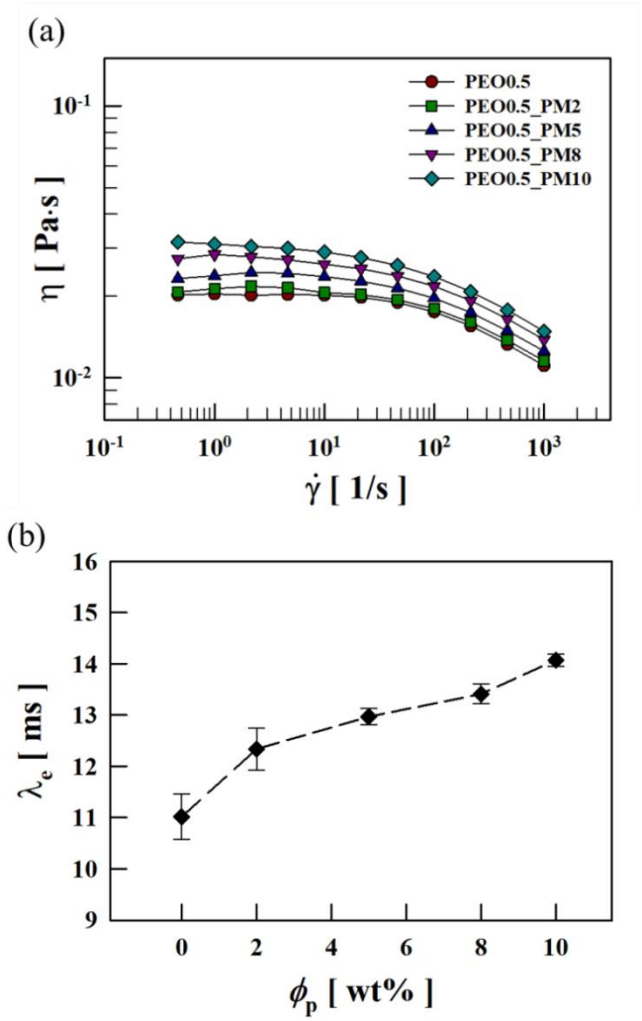

Figure 3. Rheological properties of PMMA/PEO suspensions with various PMMA particle weight fractions ($\boldsymbol{\phi_p}$); 0, 2, 5, 8, 10 wt%; (a) shear-viscosity as a function of shear rate ($\dot{\boldsymbol{\gamma}}$); (b) extensional relaxation time ($\boldsymbol{\lambda_e}$) as a function of particle weight fraction ($\boldsymbol{\phi_p}$)

3.1.2. Capillary thinning process

Fig.4 shows the capillary thinning process of PEO0.5 and PEO0.5_PM10. For both cases, in the elasto-capillary stage polymeric filament was formed and its diameter decayed exponentially, and then in the instability stage blistering pattern appeared on the filament. However, the duration of each stage and the time at which the instability appeared was different for both samples. For PEO0.5, the constriction at neck, which is called breathing, became evident at the end of the elasto-capillary stage, approximately 60 ms after the stage had begun. Subsequently, we observed the 1st bead at 84 ms, which led to the blistering pattern roughly at 96 ms. PEO0.5_PM10, meanwhile, showed the evident constriction by breathing approximately at 72 ms and the 1st bead at 96 ms. Then, well-developed blistering pattern appeared at 108 ms. Likewise, as the addition of particles elevated viscosity and extensional relaxation time (Fig.3), the elasto-capillary stage of PEO0.5_PM10 lasted longer than that of PEO.05 and the distinctive instability features such as breathing, the 1st bead and blistering appeared later for PEO0.5_PM10. However, with the introduction of t^* in section 2.3.2., we confirmed that breathing and the 1st bead appeared earlier for the particulate system in view of the progression of capillary thinning. Details will be discussed in later sections. Once the instability appeared, the process in the instability stage of PEO0.5_PM10 accelerated and took less time to reach the final break-up. In addition, the position of the 1st bead was not the same for both systems. The 1st bead appeared near the upper neck for PEO0.5, while at the lower half of the filament for PEO0.5_PM10. The added particles did not change the thinning dynamics of polymer solution, but

affected the duration of each stage and the instability pattern.

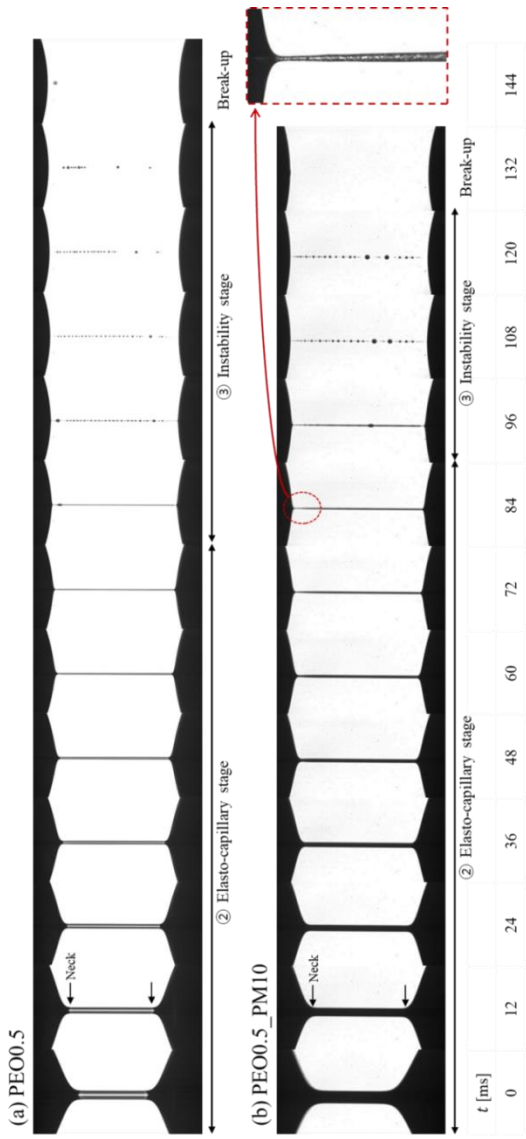

Figure 4. The capillary thinning process for (a) PEO0.5 and (b) PEO0.5_PM10. Each frame shows the evolution of every 12 ms. The first frame denotes the point at which the elasto-capillary stage begins with the formation of a polymeric filament and the last frame is the point at which the final break-up happens. The neck which connects the filament and the drop is marked with an arrow. For the image of PEO0.5_PM10 at $t = 84$ ms, the magnified image shows a well-developed constriction at the neck by breathing effect.

3.2. Breathing effect

3.2.1. Effect of the particle addition

Constriction at the neck (Fig.4) in the later elasto-capillary stage is called “breathing,” which is known to trigger the transition from the elasto-capillary stage to the instability stage [20, 30]. In order to quantitatively analyze breathing, we compared the diameter at the central part of the filament (D_{fila}) and the diameter at the neck (D_{min}). Fig.5 (a) shows the evolution of D_{min}/D_{fila} as a function of t^* which represents the progression of capillary thinning, and Fig.5 (b) shows the change of t^* required for D_{min} to be reduced to 70% of D_{fila} (t^*_{brth}) so as to monitor the development of breathing.

For pure PEO solution without particle, there was little difference in D_{min} and D_{fila} before breathing took place. That is, D_{min}/D_{fila} remained almost unity in the range of $0.0 \leq t^* \leq 0.8$. However, when the constriction occurred at the neck due to breathing, D_{min} became smaller than D_{fila} and D_{min}/D_{fila} went below unity (Fig.5 (a)). As more particles were dispersed, D_{min} deviated more rapidly from D_{fila}. When 10 wt% of particles were added, t^*_{brth} dropped 26.1% from 2.07 to 1.53. With the increase in the particle concentration, breathing became apparent at earlier t^* or at less progression of capillary thinning.

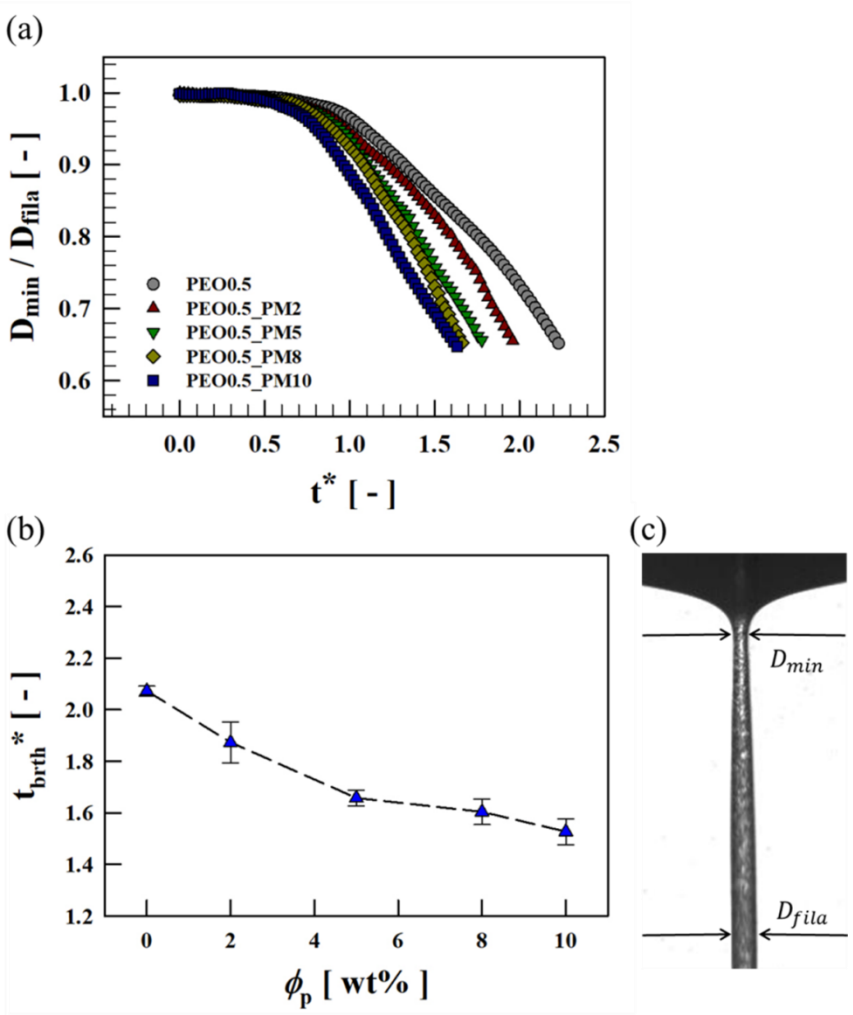

Figure 5. Breathing of PMMA/PEO suspensions: (a) the ratio of $\boldsymbol{D_{min}}$ and $\boldsymbol{D_{fila}}$ as a function of the progression of capillary thinning ($\boldsymbol{t}^*$); (b) the specific $\boldsymbol{t}^*$ required for $\boldsymbol{D_{min}}$ to be reduced to 70% of $\boldsymbol{D_{fila}}$ ($\boldsymbol{t^*_{brth}}$); (c) a shadowgraph image for PEO0.5_PM10 at $\boldsymbol{t^*_{brth}}$

3.2.2. Effect of the elevation in viscosity

The dynamics of capillary thinning of polymer solution is determined by the balance between squeezing effect by capillary pressure and resistance against it which originates from viscous and elastic stress. Increasing particle concentration leads to the elevation of the viscosity which helps the sample fluid to resist against the thinning process. Nevertheless, the experimental results showed that the addition of particle rather enhanced breathing. In order to discriminate and evaluate the effect of the elevation in viscosity due to particle addition on breathing, Gly/PEO solutions which were viscosity-matched with PMMA/PEO suspensions were prepared and tested. Pre-calculated amount of glycerin was added in PEO solution to match the elevation in viscosity. Each pair had the same viscosity, surface tension and polymer concentration. The D_{min}/D_{fila} profiles of Gly/PEO solutions were presented in Fig.6 (a). PEO0.5_PM2 was able to be paired to PEO0.5_Gly7, PEO0.5_PM5 to PEO0.5_Gly13, PEO0.5_PM8 to PEO0.5_Gly22 and PEO0.5_PM10 to PEO0.5_Gly27, respectively (Table 2). When the particle concentration of PMMA/PEO suspension increased up to 10 wt%, t^*_{brth} dropped to 1.53 from 2.07. On the other hand, t^*_{brth} of Gly/PEO solutions remained constant regardless of their glycerin fraction, or zero-shear viscosity (Fig.6 (b)). That is, the change in viscosity had little effect on breathing.

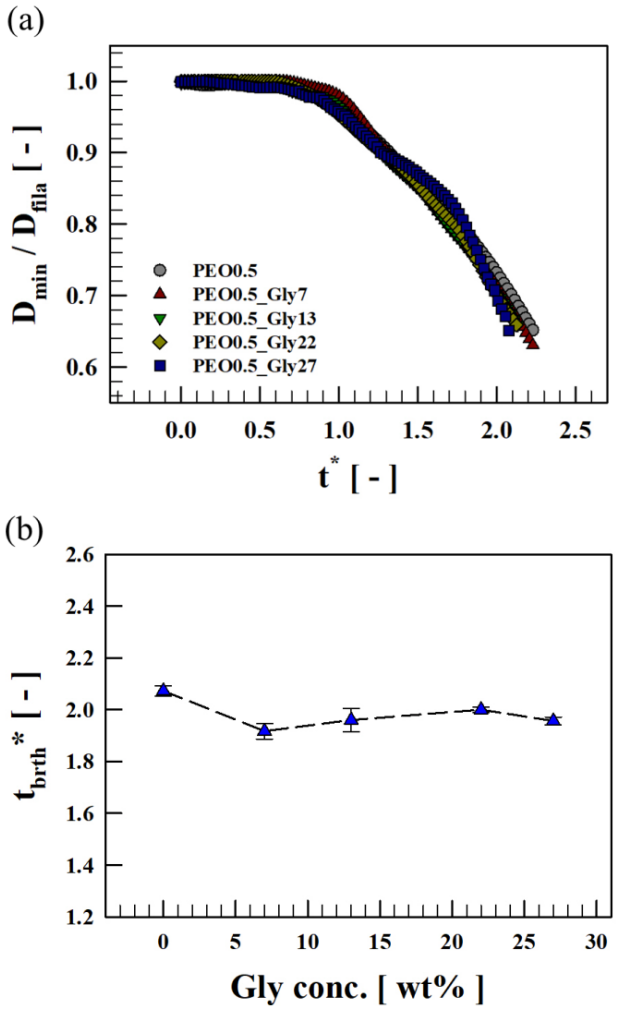

Figure 6. Breathing of Gly/PEO solutions: (a) the ratio of $\boldsymbol{D_{min}}$ and $\boldsymbol{D_{fila}}$ as a function of progression of capillary thinning ($\boldsymbol{t^*}$); (b) the specific $\boldsymbol{t^*}$ required for $\boldsymbol{D_{min}}$ to be reduced to 70% of $\boldsymbol{D_{fila}}$ ($\boldsymbol{t^*_{brth}}$)

Table 2. Properties of Gly/PEO solution; $\boldsymbol{\eta_0}$ is the zero-shear viscosity, $\boldsymbol{\lambda_e}$ is the extensional relaxation time, and $\boldsymbol{\sigma}$ is the surface tension

Name	PEO conc. $[wt\%]$	Gly conc. $[wt\%]$	$\eta_0\ [cP]$	$\lambda_e\ [ms]$	$\sigma\ [mN/m]$	Viscosity-matched
PEO0.5		0	19.9	11.02	60.55	
PEO0.5_Gly7		7	20.7	13.04	59.17	PEO0.5_PM2
PEO0.5_Gly13	0.5	13	22.7	14.13	59.17	PEO0.5_PM5
PEO0.5_Gly22		22	28.1	19.06	59.00	PEO0.5_PM8
PEO0.5_Gly27		27	29.6	22.26	58.14	PEO0.5_PM10

3.2.3. Role of the extensional property

Considering that the change in viscosity had little effect on breathing and the surface tension was practically identical for all PMMA/PEO suspensions, it could be thought that the change in breathing originated from the effect of particles on the extensional properties which resulted from the extension of polymer chains under extensional flow. PMMA/PEO suspension had smaller extensional relaxation time than that of its counterpart Gly/PEO solution as in Fig.7 (a), and the difference increased with particle concentration. Particle addition also altered extensional viscosity. Extensional viscosity of PEO0.5_PM2 and PEO0.5_Gly7 is compared in Fig.7 (b), and PEO0.5_PM10 and PEO0.5_Gly27 in Fig.7 (c). Both PEO0.5_PM2 and PEO0.5_PM10 showed a smaller extensional viscosity than that of their counterpart Gly/PEO solutions, and the difference increased with particle concentration. In summary, the presence of particles disturbed the extension of polymer chain under extensional flow, lowering the extensional viscosity and relaxation time compared to its counterpart (viscosity-matched) Gly/PEO solution.

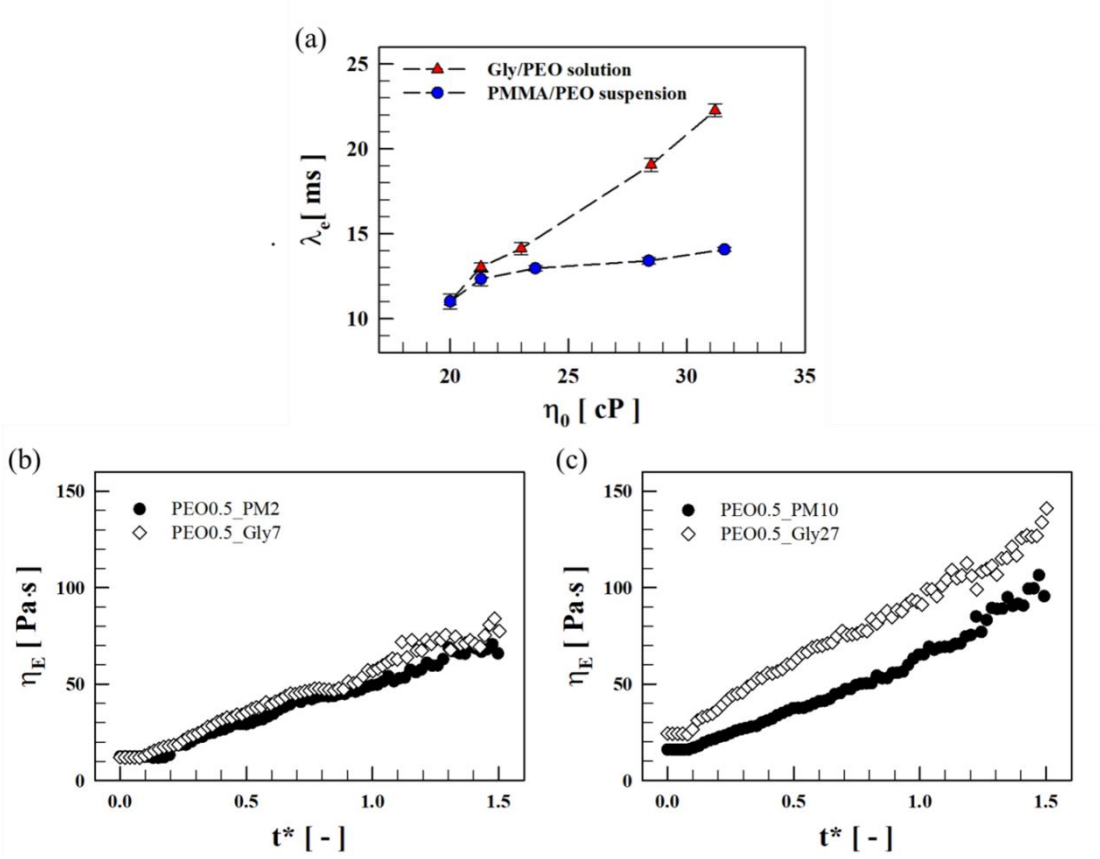

Figure 7. Comparison of the extensional properties for PMMA/PEO suspension and Gly/PEO solution: (a) extensional relaxation time ($\boldsymbol{\lambda_e}$) as a function of zero shear viscosity ($\boldsymbol{\eta_0}$), which varies with PMMA particle and glycerin weight fraction; (b) extensional viscosity ($\boldsymbol{\eta_E}$) of PEO0.5_PM2 and PEO0.5_Gly7; (c) extensional viscosity ($\boldsymbol{\eta_E}$) of PEO0.5_PM10 and PEO0.5_Gly27

Strain hardening parameter, a ratio of the extensional viscosity at high strain rate ($\bar{\eta}_{e,high}$) to the extensional viscosity at low strain rate ($\bar{\eta}_{e,low}$), shows the extent of strain hardening effect arisen by the chain stretch under extensional flow [31-33]. In this paper, $\bar{\eta}_{e,low}$ was defined as the extensional viscosity at the Newtonian stage which is three times the zero shear viscosity because the fluid can be considered as a Newtonian fluid during the stage. $\bar{\eta}_{e,high}$ was defined as the extensional viscosity at $t^* = 0$ when the elasto-capillary stage begins with the formation of the filament.

$$\zeta = \frac{\bar{\eta}_{e,high}}{\bar{\eta}_{e,low}} = \frac{\bar{\eta}_e(t^* = 0)}{3\eta_0} \tag{6}$$

Strain hardening parameter of Gly/PEO solution increased with glycerin concentration, while that of PMMA/PEO suspension decreased with particle concentration (Fig.8). As previous study showed [25], shear flow component generated at the boundary of the particle disturbed the stretching of adjacent polymer chains, lowering extensional properties. Even though a pair of PMMA/PEO suspension and Gly/PEO solution had the same bulk properties, the behavior of polymer chains under extensional flow is not the same, inducing different degree of strain hardening.

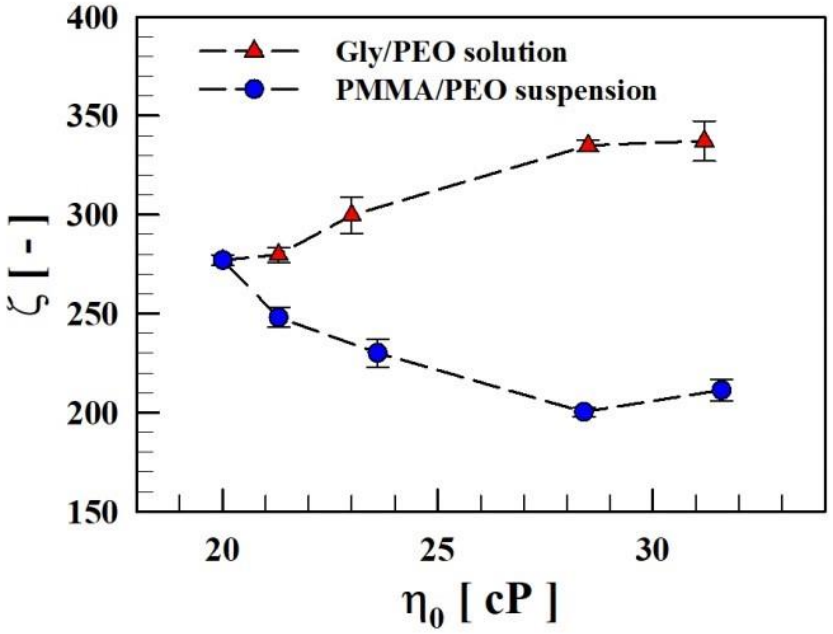

Figure 8. Strain hardening parameter ($\boldsymbol{\zeta}$) of PMMA/PEO suspension and Gly/PEO solution as a function of zero-shear viscosity ($\boldsymbol{\eta_0}$), which varies with PMMA particle weight fraction and glycerin concentration

As the breathing is closely related to the behavior of polymer chains under extensional flow, particles also can alter its outbreak pattern. Polymer chains are stretched inside the filament where strong extensional flow is dominant, and then they recoil back to the relaxed state at the drop where the flow dissipates. At the neck, the transition of the state of polymer arises and the elastic stress cannot sufficiently resist against the capillary pressure, resulting in a slight constriction, i.e. breathing. According to the experimental results, inhibition on stretching motion of polymer chains by particles promoted breathing. As particle concentration increased, the inhibition on the extension of polymer chain became severe, causing the breathing with less progression of capillary thinning.

3.3. Formation of the 1st bead

3.3.1. Effect of the particle addition on t^*

Iterated beads were formed on the filament almost simultaneously within a few milliseconds after breathing triggered the transition to the instability stage. The initiation of blistering could be confirmed by the formation of the 1st bead. We could detect the formation of the 1st bead by measuring the standard deviation of diameters along the filament. In order to calculate the standard deviation, the edge of free surface of the filament was detected from the image by using MATLAB and ther time evolution of free surface was able to be analyzed systemically. As the filament maintained its axially uniform cylindrical shape before the formation of the 1st bead, the standard deviation was small; approximately 0.4 μm. The standard deviation drastically increased at the moment the bead appeared. In this paper, we defined t^*_{bead} as the point at which the standard deviation of the diameter jumped above 1 μm, indicating the 1st bead formation.

Fig.9 (a) shows the evolution of the standard deviation of filament diameter as a function of t^*. Breathing of PMMA/PEO suspension became evident in the range of $1.53 \leq t^* \leq 2.07$, depending on particle concentration. Then, the 1st bead appeared and broke the uniform cylindrical shape of the filament in the range of $2.22 \leq t^* \leq 2.74$, increasing the standard deviation of diameter significantly. As the particle concentration increased to 10 wt%, t^*_{bead} dropped 19% from 2.74 to 2.22. It means that the 1st bead appeared at earlier t^*, i.e. less progression of capillary thinning, with the increase in particle concentration (Fig.9 (b)).

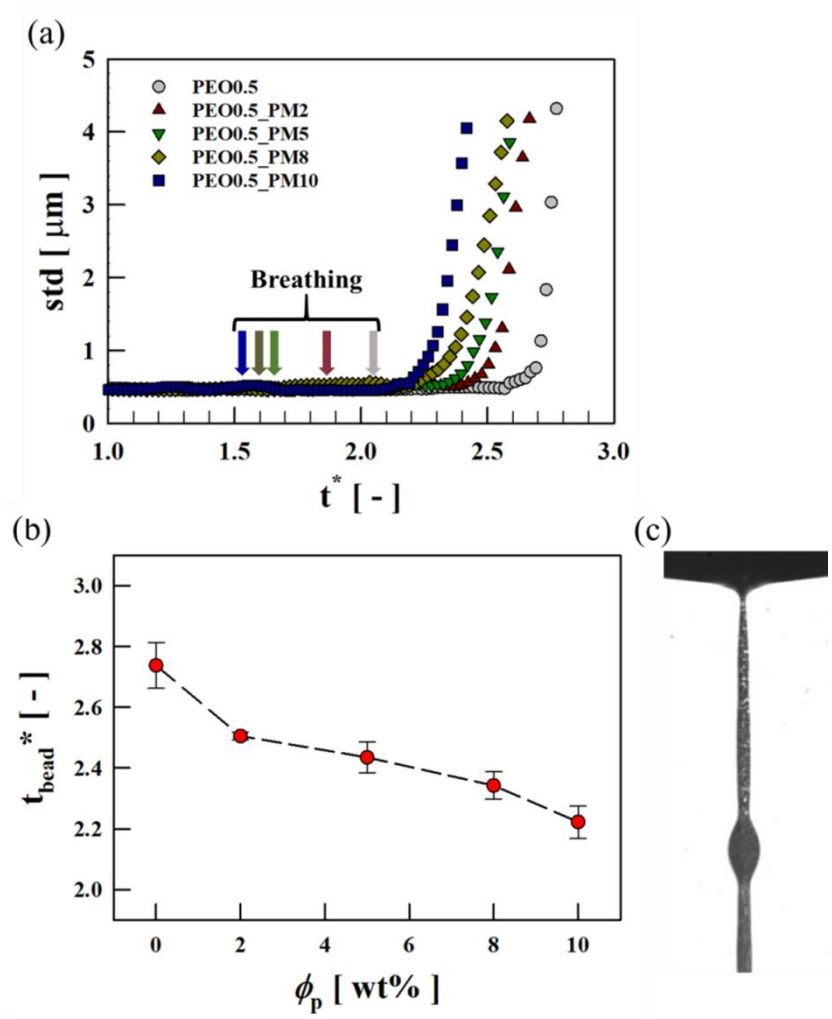

Figure 9. Change of free surface by the bead formation of PMMA/PEO suspensions: (a) evolutions of standard deviation of diameters (***std***) as a function of the progression of capillary thinning ($\boldsymbol{t}^*$). Arrows matched with symbol colors represent $\boldsymbol{t}^*_{\boldsymbol{brth}}$ of each sample ($\boldsymbol{t}^*_{\boldsymbol{brth}} = \mathbf{2.07}$ for PEO0.5, $\mathbf{1.87}$ for PEO0.5_PM2, $\mathbf{1.66}$ for PEO0.5_PM5, $\mathbf{1.60}$ for PEO.5_PM8, and $\mathbf{1.53}$ for PEO0.5_PM10); (b) the specific $\boldsymbol{t}^*$ required for the standard deviation to jump above 1 μm ($\boldsymbol{t}^*_{\boldsymbol{bead}}$); (c) a shadowgraph image for PEO0.5_PM10 at $\boldsymbol{t}^*_{\boldsymbol{bead}}$.

As in section 3.2.2., we compared the 1st bead formation of four Gly/PEO solutions which were viscosity-matched to PMMA/PEO suspensions to discriminate and evaluate the effect of the elevation in viscosity by the particle addition. The standard deviation curves for Gly/PEO solutions surprisingly overlapped into a single curve regardless of glycerin concentration (Fig.10 (a)), and the t^*_{bead} remained almost constant regardless of glycerin concentration (Fig.10 (b)). Thus, we can say that the viscosity elevation by the particle addition barely affects the 1st bead formation. Breathing was followed by the formation of 1st bead because the constriction arouses the difference in capillary pressure between the neck and the region around it, leading to the inhibition on the flow passing through the neck. Therefore, it is not surprising that the early occurrence of breathing due to the addition of particles leads to the early appearance of the 1st bead.

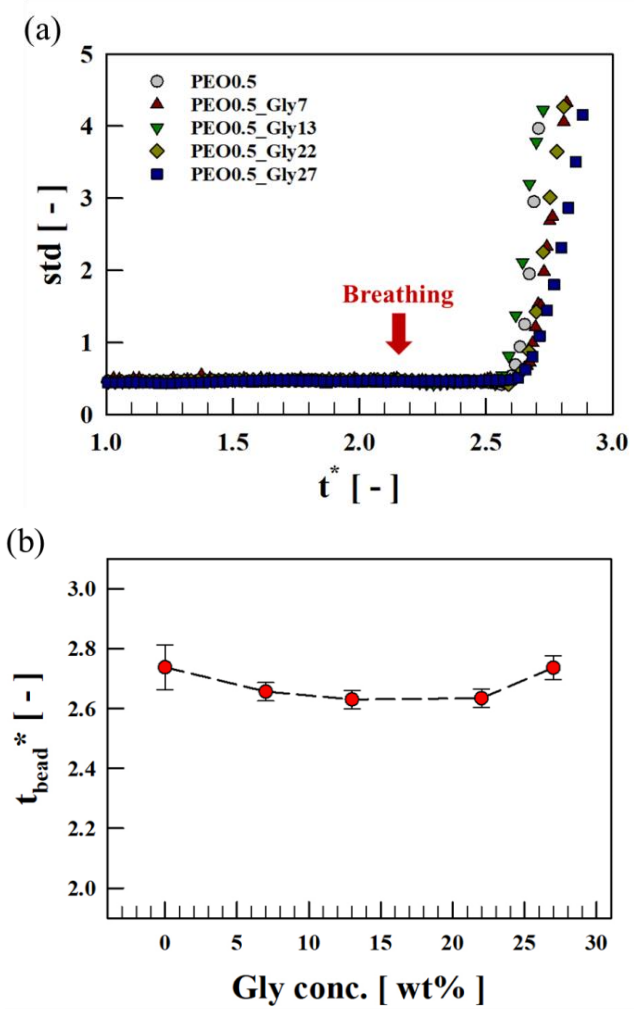

Figure 10. Change of free surface by the bead formation of Gly/PEO suspensions: (a) evolutions of standard deviation of diameters (***std***) as a function of the progression of capillary thinning ($\boldsymbol{t^*}$). An arrow indicates $\boldsymbol{t^*_{brth}}$ of PEO0.5 ($\boldsymbol{t^*_{brth} = 2.07}$); (b) the specific $\boldsymbol{t^*}$ required for the standard deviation to jump above 1 μm ($\boldsymbol{t^*_{bead}}$)

3.3.2. Effect of the particle addition on position

The addition of particles also influenced the position of the 1st bead. Fig.11 (a) shows a histogram of the distribution of the 1st bead positions for PEO0.5, PEO0.5_PM2 and PEO0.5_PM10. L_0 is the length of the entire filament connecting two drops, and L_i is the length from the lower drop to the 1st bead. For each sample, one hundred tests were conducted to obtain the reliable distribution of the 1st bead position. In case of PEO0.5, a pure PEO solution without particles, for 72 out of 100 tests the 1st bead was formed near the upper neck corresponding to 90% of the filament length. When 2 wt% of particles were added, although the number of the 1st beads formed at the position of 90% of the filament length decreased to 50 out of 100 tests, the overall tendency of the bead position was similar to that of PEO0.5. However, when the particle concentration increased to 10 wt%, the tendency completely changed. As shown in Fig.11 (b), for PEO0.5_PM10, the 1st bead could appear anywhere on the filament; upper, central and lower part of the filament with similar probability. With the increase in particle concentration, the position of the 1st bead became more random.

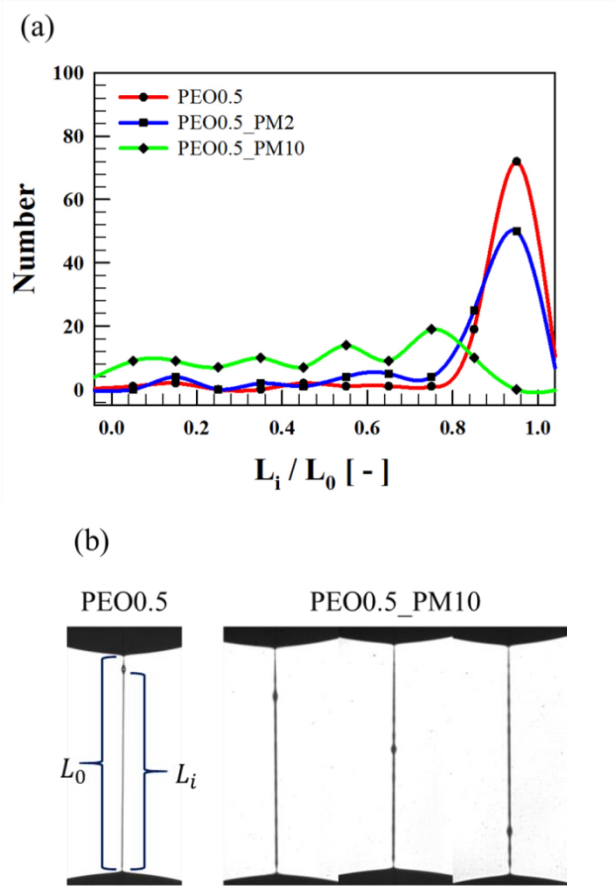

Figure 11. The position of the 1st beads: (a) histogram of the distribution of the position of the 1st bead for PEO0.5, PEO0.5_PM2 and PEO0.5_PM10. Hundred experiments were conducted for each case; (b) shadowgraph images of the filaments which shows the 1st bead for PEO0.5 and PEO0.5_PM10

Particles confined inside the filament where strong extensional flow is predominant are not uniformly distributed, and this non-uniform distribution of particles induces heterogeneity in the final stage of the filament break-up process [11]. In order to quantify the distribution of the particles inside the filament, the light intensity of the filament was measured. As the backlight is blocked by particles, particle-rich region is dark while particle-poor region is bright. That is, we can estimate the local particle concentration inside the filament by measuring the light intensity from the image. The light intensity was too noisy so it was filtered with Fourier transform to get a clear curve; zero assigned to the darkest black color and one assigned to the brightest color. We calculated the light intensity at each height by averaging the light intensity of adjacent 3 ~ 5 pixels at the same height.

As shown in Fig.12 (a), although the filament maintained its cylindrical shape at $t^* = 2.00$, the particle distribution inside was not uniform at all, and the fluctuation of the local particle concentration grew as the thinning proceeded. The part with more particles were thicker than the part with less particles, which induced non-uniform filament shape [12]. As a result, the particle-rich region developed to a bead and the particle-poor region became the liquid bridge connecting the beads. In Fig. 12 (b), the arrows indicate the regions with high local particle concentration, and they finally developed to beads as the capillary thinning proceeded. Particle-rich region can be located randomly with the fluctuation of local particle concentration. Thus, randomization of position of the 1st bead was attributed to the non-uniform particle distribution inside the filament.

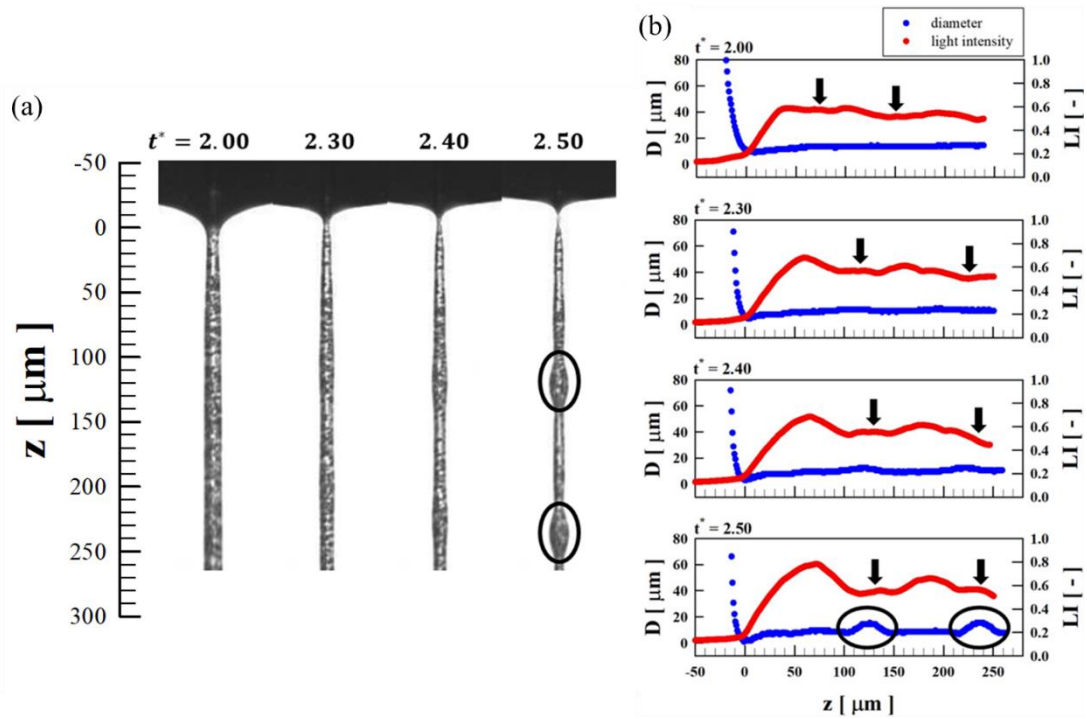

Figure 12. Local particle concentration inside the filament: (a) capillary thinning process of PEO0.5_PM5; (b) evolution of light intensity (***LI***) and diameter of filament (***D***). The position of neck is set as $z = 0$

4. Conclusion

In this study, we investigated the effect of particles on breathing and the 1st bead formation in capillary thinning of PMMA/PEO suspension. As more particles were added to PEO solution, the breathing and the 1st bead appeared at earlier t^*, which means that the transition to the instability stage occurred earlier with less progression of the capillary thinning process. We found out that the effect of particles on the instability is irrelevant to the elevation in viscosity by comparing the instability patterns of Gly/PEO solutions which were viscosity-matched with PMMA/PEO suspensions. In addition, PMMA/PEO suspension had smaller extensional relaxation time and viscosity than those of its counterpart Gly/PEO solution. That is, even though each pair of PMMA/PEO suspension and Gly/PEO solution had the same viscosity, surface tension and polymer concentration, the behavior of polymer chains under extensional flow was not the same. As the extension of polymer chains was inhibited by the added particles, the breathing took place with less progression of capillary thinning. Subsequently, the 1st bead also appeared with less progression of capillary thinning process because the early occurrence of breathing led to the early formation of the bead.

The addition of particles altered the position of the 1st bead. When 2 wt% of particles were added, there was little change in the position of the 1st bead compared to the sample without particle. However, when the particle concentration increased up to 10 wt%, the 1st bead could appear anywhere on the filament, changing the tendency completely. Randomized position of the 1st bead was attributed to the non-uniform

particle distribution inside the thinning filament. The local particle concentration fluctuated with the thinning of the filament. The particle-rich region developed to a bead, while the particle-poor region became liquid bridge connecting the beads.

In conclusion, the addition of particles accelerated the transition to the instability stage from the elasto-capillary stage, inducing complex patterns of instability. With the addition of particles, breathing and the 1^{st} bead formation appeared with less progression of the capillary thinning, and the position of the 1^{st} bead became random due to the fluctuation of the local particle concentration inside the filament. When we treat the complex fluid which consists of even a small amount of particles, the bulk properties may not be enough for understanding the dynamics of its flow, especially in extensional flow field.

References

1. Lee, J., et al., *A new paradigm of materials processing—heterogeneity control.* Current Opinion in Chemical Engineering, 2017. **16**: p. 16-22.
2. Echendu, S.O.S., H.R. Tamaddon-Jahromi, and M.F. Webster, *Modelling polymeric flows in reverse roll coating processes with dynamic wetting lines and air-entrainment: FENE and PTT solutions.* Journal of Non-Newtonian Fluid Mechanics, 2014. **214**(Supplement C): p. 38-56.
3. Fernando, R.H., L.L. Xing, and J.E. Glass, *Rheology parameters controlling spray atomization and roll misting behavior of waterborne coatings.* Progress in Organic Coatings, 2000. **40**(1): p. 35-38.
4. Jo, B.W., et al., *Evaluation of jet performance in drop-on-demand (DOD) inkjet printing.* Korean Journal of Chemical Engineering, 2009. **26**(2): p. 339-348.
5. Hong, J.S. and C. Kim, *Dispersion of multi-walled carbon nanotubes in PDMS/PB blend.* Rheologica Acta, 2011. **50**(11-12): p. 955-964.
6. Kim, H.J. and I.C. Um, *Relationship between rheology and electro-spinning performance of regenerated silk fibroin prepared using different degumming methods.* Korea-Australia Rheology Journal, 2014. **26**(2): p. 119-125.
7. Bousfield, D.W., et al., *Nonlinear analysis of the surface tension driven breakup of viscoelastic filaments.* Journal of Non-Newtonian Fluid Mechanics, 1986. **21**(1): p. 79-97.
8. Fong, H., I. Chun, and D.H. Reneker, *Beaded nanofibers formed*

during electrospinning. Polymer, 1999. **40**(16): p. 4585-4592.

9. Christanti, Y. and L.M. Walker, *Surface tension driven jet break up of strain-hardening polymer solutions.* Journal of Non-Newtonian Fluid Mechanics, 2001. **100**(1): p. 9-26.
10. Moon, J.Y., et al., *Filament thinning of silicone oil/poly(methyl methacrylate) suspensions under extensional flow.* Rheologica Acta, 2015. **54**(8): p. 705-714.
11. Moon, J.Y., et al., *Heterogeneity in the final stage of filament breakup of silicone oil/PMMA suspensions.* Rheologica Acta, 2016. **55**(2): p. 91-101.
12. Furbank, R.J. and J.F. Morris, *Pendant drop thread dynamics of particle-laden liquids.* International Journal of Multiphase Flow, 2007. **33**(4): p. 448-468.
13. Alexandrou, A.N., et al., *Breakup of a capillary bridge of suspensions.* Fluid Dynamics, 2010. **45**(6): p. 952-964.
14. McKinley, G.H., *Visco-elasto-capillary thinning and break-up of complex fluids.* Rheology Reviews, 2005.
15. Anna, S.L. and G.H. McKinley, *Elasto-capillary thinning and breakup of model elastic liquids.* Journal of Rheology, 2001. **45**(1): p. 115-138.
16. Campo-Deaño, L. and C. Clasen, *The slow retraction method (SRM) for the determination of ultra-short relaxation times in capillary breakup extensional rheometry experiments.* Journal of Non-Newtonian Fluid Mechanics, 2010. **165**(23): p. 1688-1699.
17. Keshavarz, B., et al., *Studying the effects of elongational properties on atomization of weakly viscoelastic solutions using Rayleigh Ohnesorge Jetting Extensional Rheometry (ROJER).*

Journal of Non-Newtonian Fluid Mechanics, 2015. **222**(Supplement C): p. 171-189.

18. Oliveira, M.S.N. and G.H. McKinley, *Iterated stretching and multiple beads-on-a-string phenomena in dilute solutions of highly extensible flexible polymers.* Physics of Fluids, 2005. **17**(7): p. 071704.
19. Clasen, C., et al., *The beads-on-string structure of viscoelastic threads.* Journal of Fluid Mechanics, 2006. **556**: p. 283-308.
20. Sattler, R., C. Wagner, and J. Eggers, *Blistering Pattern and Formation of Nanofibers in Capillary Thinning of Polymer Solutions.* Physical Review Letters, 2008. **100**(16): p. 164502.
21. Lim, S., et al., *The effect of binders on the rheological properties and the microstructure formation of lithium-ion battery anode slurries.* Journal of Power Sources, 2015. **299**(Supplement C): p. 221-230.
22. Kwon, O.M., et al., *Interplay between structure and property of graphene nanoplatelet networks formed by an electric field in a poly(lactic acid) matrix.* Journal of Rheology, 2017. **61**(2): p. 291-303.
23. Batchelor, G.K., *The stress generated in a non-dilute suspension of elongated particles by pure straining motion.* Journal of Fluid Mechanics, 1971. **46**(4): p. 813-829.
24. Ryskin, G., G. Ryskin, and J.M. Rallison, *The extensional viscosity of a dilute suspension of spherical particles at intermediate microscale Reynolds numbers.* Journal of Fluid Mechanics, 1980. **99**(3): p. 513-529.
25. Han, H. and C. Kim, *Extensional behavior of rod suspension in dilute polymer solution.* Korea-Australia Rheology Journal,

2015. **27**(3): p. 197-206.

26. Rodd, L.E., et al., *Capillary break-up rheometry of low-viscosity elastic fluids.* Applied Rheology, 2005. **15**(1): p. 12-27.
27. Spiegelberg, S.H. and G.H. McKinley, *Stress relaxation and elastic decohesion of viscoelastic polymer solutions in extensional flow.* Journal of Non-Newtonian Fluid Mechanics, 1996. **67**: p. 49-76.
28. Rasmussen, H.K. and O. Hassager, *The role of surface tension on the elastic decohesion of polymeric filaments.* Journal of Rheology, 2001. **45**(2): p. 527-537.
29. Clasen, C., et al., *How dilute are dilute solutions in extensional flows?* Journal of Rheology, 2006. **50**(6): p. 849-881.
30. Sattler, R., et al., *The final stages of capillary break-up of polymer solutions.* Physics of Fluids, 2012. **24**(2): p. 023101.
31. Le Meins, J.-F., P. Moldenaers, and J. Mewis, *Suspensions of monodisperse spheres in polymer melts: particle size effects in extensional flow.* Rheologica Acta, 2003. **42**(1): p. 184-190.
32. Kobayashi, M., et al., *Influence of glass beads on the elongational viscosity of polyethylene with anomalous strain rate dependence of the strain-hardening.* Polymer, 1996. **37**(16): p. 3745-3747.
33. Hong, J.S., K.H. Ahn, and S.J. Lee, *Strain hardening behavior of linear polymer melts.* Korea Australia Rheology Journal, 2004. **16**(4): p. 213-218.

국문 초록

본 연구는 고분자용액에 분산된 입자가 신장유동 하에서 현탁액의 신장거동에 미치는 영향에 대하여 논하였다. 특히, 불안정 거동의 초반부에 나타나 블리스터링을 유발하는 브리딩 현상 및 첫 번째 비드 형성에 초점을 맞추었다. 고분자용액 신장 시 발생하는 필라멘트의 끊김 공정을 관찰함으로써 필라멘트 표면에 발생하는 불안정 거동에 대한 PMMA 입자의 영향을 연구하였다. 첨가된 입자는 브리딩 현상의 발현과 첫 번째 비드의 형성을 촉진한다. 그 원인을 판단하기 위해 PMMA/PEO 현탁액과 점도, 표면장력, 고분자농도 등의 물성이 매칭된 Glycerin/PEO 용액을 제작하여 그 불안정 거동 양상을 비교하였다. 이를 통해 첨가된 입자가 신장유동 하에서 고분자 사슬의 신장을 방해하면 브리딩 현상이 촉진되고, 이어서 첫 번째 비드 형성 역시 촉진됨을 확인하였다. 더불어 입자의 첨가는 첫 번째 비드의 위치에도 영향을 미친다. 입자가 첨가되지 않은 순수한 고분자용액과 소량(~2 wt%)의 입자를 함유한 고분자용액의 경우에는 첫 번째 비드가 주로 상단부의 넥 근처에서 형성된다. 그러나, 입자 함량이 10 wt%까지 증가하면 비드는 상단부 넥 근처에 국한되지 않고 필라멘트의 다양한 위치에서 나타날 수 있게 된다. 이러한 비드 위치의 임의성 증대는 필라멘트 내부의 불균일한 입자분포에 기인한다.